# Hydropower Systems: Comparison of Mechanistic and Table Look-up Turbine Models

Valentyna Splavska    Liubomyr Vytvytskyi    Bernt Lie

University College of Southeast Norway, Porsgrunn, `bernt.lie@usn.no`, `valentyna.splavska@gmail.com`

## Abstract

In this paper, a detailed overview of hydropower system components is given. Components of the system include intake race, upstream and downstream surge tanks, penstock, turbine and draft tube. A case study which includes a Francis turbine, taken from the literature, was used. The paper presents a case study hydropower system, with models implemented in Modelica. For simplicity, compressibility of water and elasticity of pipe walls were neglected. The main aims are to compare a turbine model based on the Euler equations vs. a table look-up model, and illustrate how the surge tanks influence the transients of the system.

*Keywords: hydropower system, Modelica, mechanistic model, table look-up model, Francis turbine*

## 1 Introduction

A hydropower plant, including the waterway, energy transformation block, and the distribution grid, constitutes a complex dynamic system that we must control to operate within constraints. A hydropower plant can be divided into subsystems where several of these belong to the same class, hence an object-oriented modeling language will greatly simplify the process of setting up a model.

Mechanistic models based on physical principles are useful in that they enable simulation of hypothetical systems. Empirical models, on the other hand, require fitting to experimental data. Accurate mechanistic CFD models are too computationally intensive for transient analysis and control design. Mechanistic models of turbines based on the Euler equations are suitable for simulation of hypothetical systems, but may have too constrained model structure to allow for perfect representation. Dimensionless models and hill chart models can be fitted to experimental data, hence are considered empirical models. On the other hand, it is possible to fit empirical models to accurate CFD simulations instead of experimental data. These empirical models typically consist of look-up tables for how turbine power efficiency varies with flow rate, control input, etc.

In Section 2, the models of the various parts of the system are presented. In Section 3, some simulation results are given. Finally, some conclusions are drawn in Section 4.

## 2 Model development

Hydropower systems are diverse in terms of plant size, generating unit, the water head and plant purposes (IEA, 2012). The common primary classification of hydropower plants includes four functional classes: run-of-river plants, reservoir (or storage), diversion system and pumped storage plants. In this paper, the model of a hydropower system is developed by neglecting compressibility of water and elasticity of pipe walls. A reservoir hydropower system, consisting of intake race, upstream and downstream surge tanks, penstock, turbine and draft tube, is considered.

### 2.1 Reservoir

The reservoir is assumed as an open pond (Figure 1). The water level difference from reservoir to tail water is a determining factor for hydraulic effect of the entire system. For model simplification the water level in the reservoir is assumed as constant.
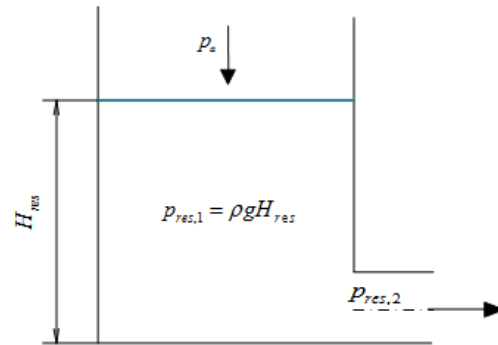


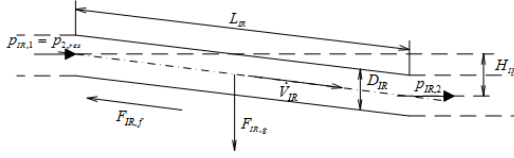**Figure 1.** Schematic representation of the model for reservoir.

The mass and momentum balances for reservoir lead to:

$$\frac{dm_{\text{res}}}{dt} = \dot{m}_{\text{i,res}} - \dot{m}_{\text{e,res}} \tag{1}$$

$$p_{\text{res},2} = p_a + \rho g H_{\text{res}} \tag{2}$$

### 2.2 Intake race

The intake race is a part of the waterway between the water intake and a surge tank, and ends with a sand trap (Figure 2). For model simplification, intake race, penstock and discharge tube are assumed as filled pipes, which leads to $\dot{m} = const$. Since the momentum flow is $\dot{\mathcal{M}} = \frac{\rho}{A}\dot{V}^2$,

**Figure 2.** Schematic representation of the model for intake race.

an assumption of the water density constancy leads to $\mathscr{M}_{\text{IR,i}} = \mathscr{M}_{\text{IR,e}}$ (Lie et al., 2016). Thus, the mass and momentum balances can be expressed as:

$$\frac{dm_{\text{IR}}}{dt} = 0 \tag{3}$$

$$\frac{d\mathscr{M}_{\text{IR}}}{dt} = F_{\text{IR}} \tag{4}$$

The forces acting on the inlet race are given as:

$$F_{\text{IR}} = F_{\text{IR,p}} + F_{\text{IR,g}} - F_{\text{IR,f}} \tag{5}$$

$$F_{\text{IR,p}} = p_{\text{IR,1}} A_{\text{IR}} - p_{\text{IR,2}} A_{\text{IR}} \tag{6}$$

$$F_{\text{IR,g}} = m_{\text{IR}} g \frac{H_{\text{IR}}}{L_{\text{IR}}} \tag{7}$$

$$\tag{8}$$

For friction forces component the Darcy description of friction is assumed:

$$F_{\text{IR,f}} = \frac{K'''_{\text{IR}} A_{\text{IR,w}} f_{\text{IR,D}}}{4} \quad A_{\text{IR,w}} = \pi D_{\text{IR}} L_{\text{IR}} \tag{9}$$

$$K'''_{\text{IR}} = \frac{\rho}{2A_{\text{IR}}^2} \dot{V}_{\text{IR}} \left| \dot{V}_{\text{IR}} \right| \tag{10}$$

Darcy's friction coefficient $f_{\text{IR,D}}$ can be given by the following explicit approximation of the implicit Colebrook model (Lie et al., 2016):

$$\frac{1}{\sqrt{f_{\text{IR,D}}}} = -2\lg\left(\frac{\varepsilon_{\text{IR}}}{3,70D_{\text{IR}}} + \frac{5,74}{N_{\text{IR,Re}}^{0,9}}\right) \tag{11}$$

$$N_{\text{Re,IR}} = \frac{\rho \dot{V}_{\text{IR}} D_{\text{IR}}}{\mu A_{\text{IR}}} \tag{12}$$

## 2.3 Manifold

The manifold connects the inlet race, the surge tank, and the penstock. by assuming that there is negligible mass (inertia) inside the manifold, steady state for both mass and momentum balances can be assumed (Lie et al., 2016). Since no mass is accumulated, the mass and momentum balances can be represented as:

$$\frac{dm_*}{dt} = 0 \tag{13}$$

$$\frac{d\mathscr{M}_*}{dt} = 0 \tag{14}$$

leading to:

$$\dot{V}_{\text{i}} = \dot{V}_{\text{P}} + \dot{V}_{\text{ST}} \tag{15}$$

$$p_{\text{IR,2}} = p_{\text{P,2}} = p_{\text{ST,1}} = p_* \tag{16}$$

## 2.4 Penstock

A penstock is a steep pipe which connects the inlet part of a hydropower system (via the manifold) and a wicket gate inlet to a turbine (Figure 3). The mass and momentum balances for the penstock:

$$\frac{dm_{\text{P}}}{dt} = 0 \tag{17}$$

$$\frac{d\mathscr{M}_{\text{P}}}{dt} = F_{\text{P}} \tag{18}$$

The forces acting on the penstock are:

$$F_{\text{P}} = F_{\text{P,p}} + F_{\text{P,g}} - F_{\text{P,f}} \tag{19}$$

$$F_{\text{P,p}} = p_{\text{P,1}} A_{\text{P}} - p_{\text{P,2}} A_{\text{P}} \tag{20}$$

$$F_{\text{P,g}} = m_{\text{P}} g \frac{H_{\text{P}}}{L_{\text{P}}} \tag{21}$$

$$F_{\text{P,f}} = \frac{K'''_{\text{P}} A_{\text{P,w}} f_{\text{P,D}}}{4} \tag{22}$$

$$A_{\text{P,w}} = \pi D_{\text{P}} L_{\text{P}} \tag{23}$$

$$K'''_{\text{P}} = \frac{\rho}{2A_{\text{P}}^2} \dot{V}_{\text{P}} \left| \dot{V}_{\text{P}} \right| \tag{24}$$

$$\frac{1}{\sqrt{f_{\text{P,D}}}} = -2\lg\left(\frac{\varepsilon_{\text{P}}}{3,70D_{\text{P}}} + \frac{5,74}{N_{\text{P,Re}}^{0,9}}\right) \tag{25}$$

$$N_{\text{Re,P}} = \frac{\rho \dot{V}_{\text{P}} D_{\text{P}}}{\mu A_{\text{P}}} \tag{26}$$

## 2.5 Surge tank

While water flow is proceeding trough the waterway, it can accelerate or decelerate causing pressure variations with magnitude exceeding the nominal pressure in the waterway, which, in its turn, leads to the load changes causing the mass oscillations called "water hammer" effect (Kjoelle, 2001; Winkler et al., 2011). The surge tank serves to reduce harmful effect of these oscillations (Figure 4). The surge tank design is an iterative process, where the stability criterions (Thoma or Svee) are the determining factors (Brekke, 2001). Since the surge tank has varying mass, the mass and momentum balances can be repre-
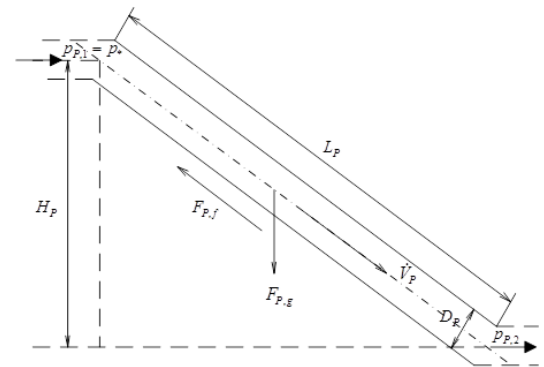


**Figure 3.** Schematic representation of the model for penstock.
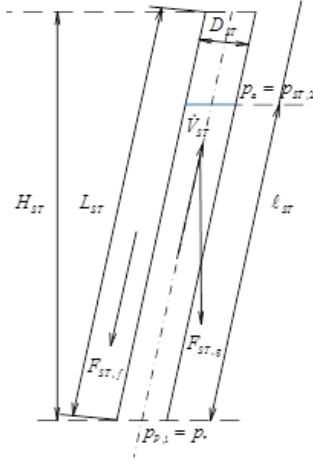
**Figure 4.** Schematic representation of the model for surge tank.

sented as:

$$\frac{dm_{\text{ST}}}{dt} = \dot{m}_{\text{ST,i}} \quad (27)$$

$$\frac{d\mathcal{M}_{\text{ST}}}{dt} = \dot{\mathcal{M}}_{\text{ST,i}} + F_{\text{ST}} \quad (28)$$

$$\mathcal{M}_{\text{ST}} = \frac{\rho}{A_{\text{ST}}} V_{\text{ST}}^2 \quad (29)$$

$$V_{\text{ST}} = \pi r_{\text{ST}}^2 \ell_{\text{ST}} = \pi \left(\frac{D_{\text{ST}}^2}{4}\right) \ell_{\text{ST}} \quad (30)$$

$$\dot{\mathcal{M}}_{\text{ST,i}} = \dot{m}_{\text{ST,i}} \upsilon = \rho \dot{V}_{\text{ST}} \upsilon = \rho \dot{V}_{\text{ST}} \frac{\dot{V}_{\text{ST}}}{A_{\text{ST}}} = \frac{\rho}{A_{\text{ST}}} \dot{V}_{\text{ST}}^2 \quad (31)$$

The forces acting in the surge tank:

$$F_{\text{ST}} = F_{\text{ST,p}} - F_{\text{ST,g}} - F_{\text{P,f}} \quad (32)$$

$$F_{\text{ST,p}} = p_{\text{ST,1}} A_{\text{ST}} - p_{\text{ST,2}} A_{\text{ST}} \quad (33)$$

$$F_{\text{ST,g}} = m_{\text{ST}} g \frac{H_{\text{ST}}}{L_{\text{ST}}} \quad (34)$$

$$F_{\text{ST,f}} = \frac{K'''_{\text{ST}} A_{\text{ST,w}} f_{\text{ST,D}}}{4} \quad (35)$$

$$A_{\text{ST,w}} = \pi D_{\text{ST}} \ell_{\text{ST}} \quad (36)$$

$$K'''_{\text{ST}} = \frac{\rho}{2A_{\text{ST}}^2} \dot{V}_{\text{ST}} |\dot{V}_{\text{ST}}| \quad (37)$$

$$\frac{1}{\sqrt{f_{\text{ST,D}}}} = -2\lg\left(\frac{\varepsilon_{\text{ST}}}{3,70 D_{\text{ST}}} + \frac{5,74}{N_{\text{ST,Re}}^{0,9}}\right) \quad (38)$$

$$N_{\text{Re,ST}} = \frac{\rho \dot{V}_{\text{ST}} D_{\text{ST}}}{\mu A_{\text{ST}}} \quad (39)$$

If the surge tank has a specific form where a cross section is a function of the elevation (Nicolet, 2007; Nicolet et al., 2007), the volume of the surge tank becomes a non-linear function of the level.

## 2.6 Discharge race

The design of the outlet tunnel is similar to the intake race tunnel (Figure 5). Additionally to assumptions considered

for the intake race, assume the transitional duct between the turbine and the inlet to the discharge race is small, so that it can be neglected.

$$\frac{dm_{\text{DR}}}{dt} = 0 \quad (40)$$

$$\frac{d\mathcal{M}_{\text{DR}}}{dt} = F_{\text{DR}} \quad (41)$$

The forces acting on the discharge race:

$$F_{\text{DR}} = F_{\text{DR,p}} + F_{\text{DR,g}} - F_{\text{DR,f}} \quad (42)$$

$$F_{\text{DR,p}} = p_{\text{DR,1}} A_{\text{DR}} - p_{\text{DR,2}} A_{\text{DR}} \quad (43)$$

$$p_{\text{DR,2}} = p_{\text{a}} + \rho g H_{\text{TW}} \quad (44)$$

$$F_{\text{DR,g}} = m_{\text{DR}} g \frac{H_{\text{DR}}}{L_{\text{DR}}} \quad (45)$$

$$F_{\text{DR,f}} = \frac{K'''_{\text{DR}} A_{,w} f_{\text{DR,D}}}{4} \quad (46)$$

$$A_{\text{DR,w}} = \pi D_{\text{DR}} L_{\text{DR}} \quad (47)$$

$$K'''_{\text{DR}} = \frac{\rho}{2A_{\text{DR}}^2} \dot{V}_{\text{DR}} |\dot{V}_{\text{DR}}| \quad (48)$$

$$\frac{1}{\sqrt{f_{\text{DR,D}}}} = -2\lg\left(\frac{\varepsilon_{\text{DR}}}{3,70 D_{\text{DR}}} + \frac{5,74}{N_{\text{DR,Re}}^{0,9}}\right) \quad (49)$$

$$N_{\text{Re,DR}} = \frac{\rho \dot{V}_{\text{DR}} D_{\text{RD}}}{\mu A_{\text{RD}}} \quad (50)$$

For the entire model, we assume that $\dot{V}_{\text{DR}} = \dot{V}_{\text{P}}$, since the penstock and the discharge race belong to the same hydraulic string (Lie et al., 2016).
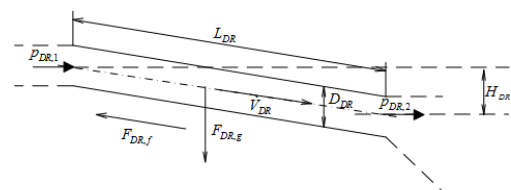
## 2.7 Francis turbine

Figure 6 illustrates absolute velocities, rotor reference velocities and relative velocities in the Francis turbine. The produced power can be given as:

$$\dot{W}_s = \dot{m}\omega\left(R_1 \frac{\dot{V}}{A_1} \cot\alpha_1 - \omega R_2^2 - R_2 \frac{\dot{V}}{A_2} \cot\beta_2\right) \quad (51)$$
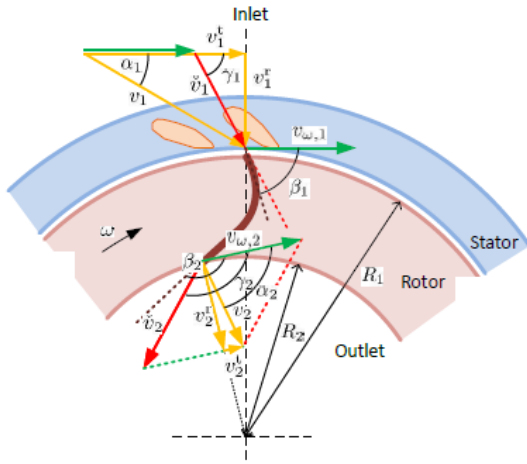
$$\dot{W}_{ft} = k_{ft,1} \dot{V} (\cot\gamma_1 - \cot\beta_1)^2 + k_{ft,2} \dot{V} \cot^2\alpha_2 + k_{ft,3} \dot{V}^2 \quad (52)$$

The total work rate removed through the turbine:

$$\dot{W}_t = \dot{W}_s + \dot{W}_{ft} + \Delta p_V \dot{V} \quad (53)$$



**Figure 5.** Schematic representation of the model for discharge race.

**Figure 6.** Key quantities in the Francis turbine model (the water effluent comes out from the paper plan; blade angles $\beta_1, \beta_2$) (Lie and Vytvytskyi, 2016).

Hence, the total pressure loss across the turbine can be found as:

$$\dot{W}_t = \Delta p_t \dot{V} \qquad (54)$$

Thus, the efficiency of the turbine can be defined as:

$$\eta = \dot{W}_s / \dot{W}_t \qquad (55)$$

# 3 Simulation results

The equation based modeling language Modelica supports differential algebraic equations, and is a good choice for modeling hydropower systems. OpenModelica is one of several free simulation tools based on Modelica; Dymola is an example of a commercial tool. Commercial hydropower libraries are available for Dymola, but a simple, free library is also under development at University College of Southeast Norway.

A case study from (Valaamo, 2016), including a Francis turbine, was used for illustration. This paper presents a case study hydropower system without surge tank, with upstream surge tank (UST) and both upstream and downstream surge tank (DST), with models implemented in Modelica (Vytvytskyi and Lie, 2016). The obtained results of turbine efficiency (Figure 7) were compared with a table look-up model (Figure 10). To make this comparison turbine efficiency was plotted with respect to volumetric flow rate (Figure 8). Pressure drop over the turbine for mentioned study cases are shown on (Figure 9).

From (Figures 7, 10), we see that a turbine model based on the Euler equations gives quite similar results to a table look-up model.
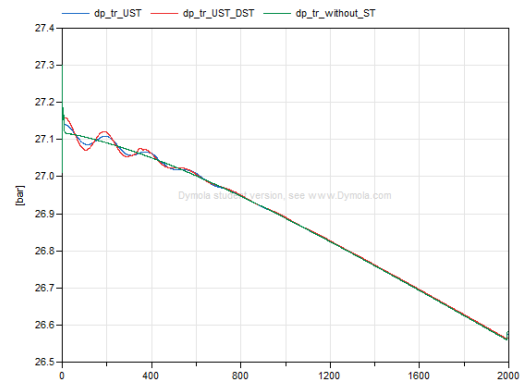
To investigate the influence of the surge tanks on the transients of the system, a ramp-up test (height=7%, duration=1$s$) was performed. Since the developed model is not suitable for analysis of cavitation, the water hammer effect is in focus.
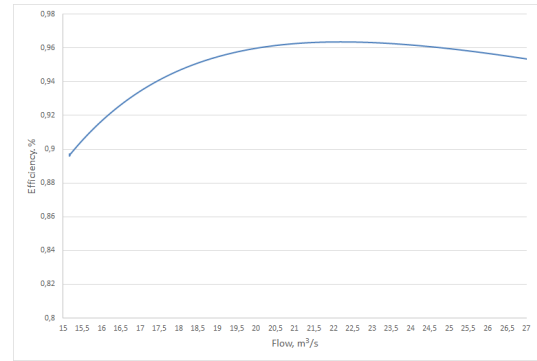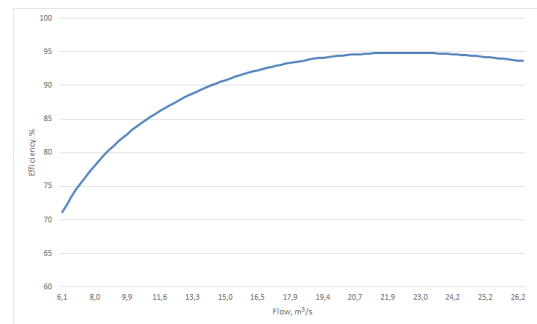


**Figure 7.** Turbine efficiency.
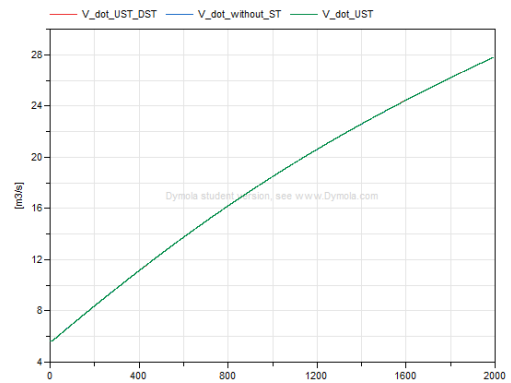


**Figure 8.** Volumetric flow rate.



**Figure 9.** Pressure drop over the turbine.



**Figure 10.** Turbine efficiency from look up table.

Figures 11, 12 show the dynamics of the inlet and outlet

pressure of the turbine for systems with surge tank and without. In the system with no surge tank, a significant pressure drop occurs. For the system with surge tank, on the other hand, the pressure oscillation is smooth (has less amplitude and magnitude), hence, the components of the system is less exposed to the harmful water hammer effect.
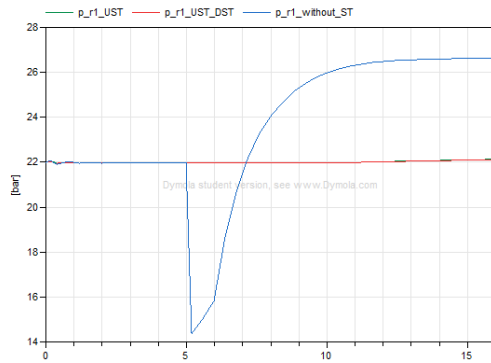


**Figure 11.** The turbine inlet pressure. Ramp-up test.
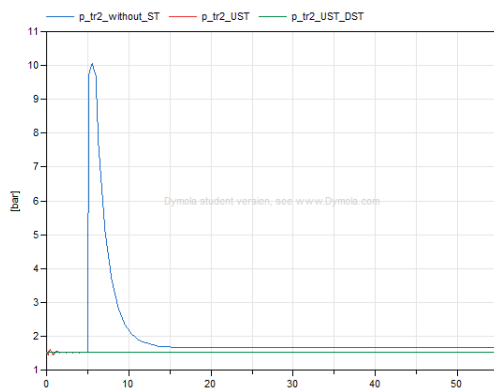


**Figure 12.** The turbine outlet pressure. Ramp-up test.

Figure 13 illustrates the dynamics of the outlet pressure of the turbine for hydropower system with one and two surge tanks to make a conclusion about feasibility of additional installation of a downstream surge tank. In the system with only upstream surge tank, the amplitude of the pressure oscillation is higher than in the system with additional downstream surge tank. Furthermore, the oscillations are smoother in the second one.

## 4 Conclusions

In this paper, a detailed overview of hydropower system components was given. A case study from the literature including a Francis turbine was used. The paper presents a case study hydropower system, with models implemented in Modelica. In this paper, a mechanistic model of the turbine based on the Euler equations was introduced, with dimensions computed using A-lab (McClimans et al., 2000). The turbine model based on the Euler equations was compared to a table look-up model. The influence of the surge tanks on the transients of the system was illustrated. The
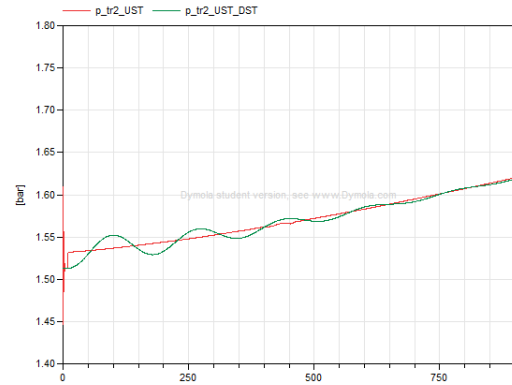


**Figure 13.** The turbine outlet pressure (cases with only upstream surge tank and both upstream and donwstream surge tanks). Step-test.

developed model may not be suitable for analysis of cavitation, since neglecting compressibility and elasticity in water/pipes filters out some pressure transients. The research contributes in refining a case study for hydropower systems, and in emphasizing the usefulness of mechanistic turbine models.

## References

H. Brekke. *Hydraulic turbines. Design, Erection and Operation*. 2001.

IEA. Technology Roadmap. Hydropower, 2012. Technical report, International energy agency, Paris Cedex, France, 2012.

A. Kjoelle. *Hydropower in Norway. Mechanical equipment. Survey*. NTNU Norwegian University of Science and Technology, 2001.

B. Lie and L. Vytvytskyi. *Modeling of Dynamic Systems. Lecture notes*. USN, 2016.

B. Lie, L. Vytvytskyi, and C. Agu. Modeling of dynamic systems. project fm 1015. *USN*, 2016.

T.A. McClimans, J. Pietrzak, V. Huess, N. Kliem, and B.O. Johannessen. A comparison of laboratory and numerical simulations of the ocean circulation in the skagerrak. *Cont. Shelf Res.*, 20:941–974, 2000.

Ch. Nicolet. *Hydroacoustic modelling and numerical simulation of unsteady operation of hydroelectric systems*. Doctor of science dissertation, EPFL Swiss Federal Institute of Technology in Lausanne, ÃĽcublens (Lausanne), Switzerland, 2007.

Ch. Nicolet, B. Greiveldinger, J.-J. HÃľrou, B. Kawkabani, P. Allenbach, J.-J. Simond, and F. Avellan. High order modeling of hydraulic power plant in islanded power network. *IEEE Transaction on Power Systems*, 22(4):1870–1892, 2007.

S.B. Valaamo. *Transient Modelling of Hydropower Plants*. Master thesis, NTNU Norwegian University of Science and Technology, Trondheim, Norway, 2016.

L. Vytvytskyi and B. Lie. Comparison of elastic vs. inelastic penstock model using openmodelica. *International Conference of Scandinavian Simulation Society, SIMS 2017*, 58, 2016.

D. Winkler, H.M. Thoresen, I. Andreassen, M.A.S. Perera, and B.R. Sharefi. Modelling and optimisation of deviation in hydro power production. *Modelica*, pages 1–10, 2011.

# Appendix A.  Parameters of the simulation

**Reservoir**

| Initial height | 48 m |
|----------------|------|
| Walls angle | 20 deg |
| Bed width | 100 m |
| Length | 500 m |
| Friction factor | 8e-4 |

**Intake**

| Height | 25 m |
|--------|------|
| Length | 2000 m |
| Diameter i&o | 5 m |

**Penstock**

| Height | 210 m |
|--------|-------|
| Length | 450 m |
| Diameter i&o | 4 m |

**Turbine**

| Diameter of the inlet pipe | 1.73 m |
|-----------------------------|--------|
| Turbine blade inlet radius | 2.02/2 m |
| Turbine blade outlet radius | 1.5/2 m |
| Radius of the guide vane susp. circle | 2.23/2 m |
| Width of turbine/blades inlet | 0.259 m |
| Width of turbine/blades outlet | 1.5/4 m |
| $r_v$ | 0.9 m |
| $r_Y$ | 1 m |
| $R_Y$ | 2.5 m |
| Hydralic friction loss coefficient | 1e5 |
| $\beta_1$ | 112 deg |
| $\beta_2$ | 163.2 deg |

**Discharge**

| Height | 5 m |
|--------|-----|
| Length | 2000 m |
| Diameter i&o | 4.5 m |

**Tail**

| Initial height | 10 m |
|----------------|------|
| Bed width | 100 m |
| Length | 500 m |
| $\alpha$ | 1145.9 deg |
| Friction factor | 8e-4 |